Plant Hormones ARTICLE

Open Access

https://doi.org/10.48130/ph-0026-0004

Plant Hormones **2026**, 2: e007

A StbZIP53-like2–StERF091 module regulates the browning of fresh-cut potatoes

Wenhui Li[#], Jixuan Cao[#], Yuan He, Yixuan Wang, Jingying Shi[*] and Zunyang Song[*]

Key Laboratory of Food Processing Technology and Quality Control in Shandong Province, College of Food Science and Engineering, Shandong Agricultural University, Tai an 271018, China

[#] Authors contributed equally: Wenhui Li, Jixuan Cao

[*] Correspondence: jyshi@sdau.edu.cn (Shi J); zunyangsong@sdau.edu.cn (Song Z)

Abstract

With the acceleration of modern life, fresh-cut potatoes (*Solanum tuberosum*) are very popular in our daily lives. However, surface browning is the major issue reducing the quality of fresh-cut potatoes during storage. Our previous study found that glutamic acid (Glu) treatment could alleviate the browning of fresh-cut potatoes; however the regulatory mechanism was still unclear. In this study, Glu treatment markedly enhanced the expression of *StbZIP53-like2*, which was a nuclear protein. StbZIP53-like2 repressed the transcriptional activity of *StPPO3*. StbZIP53-like2 cooperated with an ethylene responsive factor (ERF) transcription factor, StERF091. The transcript level of *StERF091* was also enhanced by Glu treatment, and StERF091 was a nuclear protein. Moreover, StERF091 inhibited the transcriptional activity of *StPPO2* and *StPPO3*. Moreover, the interaction of StbZIP53-like2 and StERF091 reduced the transcriptional activity of *StPPO2* and *StPPO3* compared with StbZIP53-like2 and StERF091 alone. Taken together, these results uncovered a dynamic regulatory module of StbZIP53-like2–StERF091 mediating the browning of fresh-cut potatoes.

Citation: Li W, Cao J, He Y, Wang Y, Shi J, et al. 2026. A StbZIP53-like2–StERF091 module regulates the browning of fresh-cut potatoes. *Plant Hormones* 2: e007 https://doi.org/10.48130/ph-0026-0004

Introduction

Potato (*Solanum tuberosum*) is the fourth largest food crop after corn (*Zea mays*), wheat (*Triticum aestivum*) and rice (*Oryza sativa*) in the world[1]. With the acceleration of modern life, fresh-cut potatoes have gained growing popularity in people's daily lives[2]. However, fresh-cut potatoes have several problems after cutting, such as softening, an unpleasant aroma and browning[3]. Among these problems, browning is the most common deterioration in the appearance of fresh-cut potatoes. As browning is enzymatic, it severely reduces their shelf life. When oxygen and enzymes are present, the phenolic compounds produce quinones, which then transform into pigments[4]. During the process, polyphenol oxidase (PPO) is the vital enzyme, which catalyzes not only the hydroxylation of monophenols to diphenols but also the oxidation of diphenols to quinones[1]. In recent years, many biological, chemical and physical technologies have been reported that can repress the browning of fresh-cut potatoes. Chemical technologies can significantly alleviate the browning of fresh-cut potatoes, including sulfur dioxide and sulfites, but these have food safety issues[5]. Although physical methods can effectively repress the browning of fresh-cut potatoes, these also have some issues. For example, low oxygen could markedly alleviate the browning of fresh-cut potatoes, but it leads to off-flavors and unpleasant odors[6]. Biological technologies (some natural extracts, natural edible coatings and genetic engineering technologies) can effectively inhibit the browning of fresh-cut potatoes, but most biological technologies cannot be used commercially[7]. Previous studies found that some amino acids can repress the browning of fresh-cut potatoes, including isoleucine and L-cysteine, arginine, etc.[2,8,9]. Moreover, our previous work reported that glutamic acid (Glu, $C_5H_9NO_4$) treatment markedly alleviates the browning of fresh-cut potatoes[5], but its regulatory mechanism was unclear.

According to the DNA-binding domains, transcription factors (TFs) can be classified into ethylene response factors (ERFs), WRKY transcription factors (WRKYs), NAC transcription factors (NACs), basic leucine zipper (bZIP) proteins, and so on[10]. Among them, bZIPs are named for the conserved bZIP domain, which possesses a leucine zipper dimerization domain and a basic DNA-binding domain[11]. Several studies have reported that bZIPs mediate fruit development, maturity and resistance to biotic and abiotic via directly interacting with its downstream genes[12]. For example, in apple (*Malus*) 'Pinkspire' fruit, MpbZIP9 enhances anthocyanin biosynthesis by activating *MpF3'H* expression[13]. In citrus, CsbZIP44 promotes carotenoid biosynthesis via directly activating the expression of *CsNCED2*, *CsBCH1*, *CsGGPPs* and *CsDXR*[14]. In strawberry (*Fragaria* × *ananassa*), FaTRAB1 (a bZIP transcription factor) enhances anthocyanin biosynthesis by repressing *FaMYB10* expression, which directly stimulates the expression of *FaOMT*, *FaUFGT*, *FaF3'H* and *FaANS*[15]. In pear (*Pyrus*) , PpbZIP44 promotes carbohydrate metabolism and the accumulation of flavonoids and amino acids by directly activating the transcriptional activity of *PpProDH1* and *PpSDH9*[16]. PbrbZIP15 improves the accumulation of fruit sugars by stimulating expression of the glucose isomerase gene *PbrXylA1*[17]. In banana (*Musa acuminata*), *MabZIP93* overexpression promotes fruit ripening by inducing the expression of *MaXTH23*, *MaXGT1*, *MaPE*1 and *MaPL2*[11]. Moreover, MabZIP24 promotes fruit ripening by stimulating the expression of *MaACO1*, *MaEXPA15*, *MaPE42*, *MaPE51*, *MaPL5*, *MaPL15* and *MaPG3*[18]. In sweet cherry (*Prunum avium*), PavbZIP6 enhanced fruit anthocyanin accumulation via positively regulating the expression of anthocyanin biosynthesis genes (*PavUFGT*, *PavANS* and *PavDFR*)[19]. Moreover, bZIP proteins also regulate fruit browning. PpbZIP23 and PpbZIP25 mediate the browning of peach (*Prunus persica*) fruit caused by chilling injury[12]. However, the regulatory mechanism of bZIP TFs regulate the browning of fresh-cut fruit and vegetables was still unknown.

ERFs belong to the AP2 ERF family, which is a main regulator in fruit development, maturity and ripening[20]. In tomato (*Solanum lycopersicum*), SlERF.F12 negatively mediates fruit ripening by repressing the expression of *SlACO2* and *SlACS4*[21]. SlERF.D3

negatively regulates fruit ripening and leaf senescence[22]. *SlERF.D6* overexpression promotes steroidal glycoalkaloids synthesis and fruit ripening[23]. SlERF.D7 promotes fruit ripening by activating *SlARF2* expression[24]. SlERF.F12 represses the ripening of tomato fruit by repressing the expression of *SlACS2* and *SlACS4*[21]. SlERF.C1 enhances fruits' resistance to *Botrytis cinerea* via stimulating the expression of pathogenesis-related (PR) genes[25]. In sweet cherry, PavRAV2 negatively regulates fruit size by directly repressing *PavKLUH* transcription[26]. In apple, MdERF34 can activate anthocyanin biosynthesis in the fruits[27]. MdERF4 inhibits fruit ripening via suppressing ethylene synthesis[28]. *MdERF113*-overexpression enhances fruits' cold tolerance and drought resistance[29]. In banana, MaERF95L positively mediates fruit ripening by stimulating the expression of sucrose synthesis and starch degradation genes[30]. MaERF113 promotes fruit ripening by stimulating the expression of cell, starch and chlorophyll degradation genes[31]. MaERF003 mediates fruit ripening via directly inducing the expression of chlorophyll, cell wall and starch degradation genes[32]. In peach, PpERF5 and PpERF7 increase peach fruit aroma via positively regulating *PpLOX4* expression[33]. Moreover, ERFs may mediate the browning of vegetables. CaERF4-2, CaAP2L1 and CaERF32/41/43/80/91/114 mediate the browning of sweet pepper (*Capsicum anuum*)[34]. However, the regulatory mechanism of ERFs in regulating the browning of fresh-cut fruit and vegetables is still unclear.

Herein, we found that the expression of *StbZIP53-like2* was closely associated with the browning of fresh-cut potatoes, and its expression was enhanced by Glu treatment. StbZIP53-like2 markedly repressed the expression of *StPPO2*. StbZIP53-like2 interacts with StERF091, the expression of which was increased by Glu treatment. StERF091 severely repressed the transcription of *StPPO2* and *StPPO3*. Moreover, the interaction of StERF091 and StbZIP53-like2 enhanced the transcriptional activity of *StPPO2* and *StPPO3*. Our study revealed that StbZIP53-like2–StERF091 alleviates the browning of fresh-cut potatoes by inhibiting the expression of *StPPO2* and *StPPO3*.

Materials and methods

Plant materials and treatments

Potatoes were treated via the method of Guan et al.[3]. In brief, potatoes were shredded and rinsed in a 5×10^{-5} g/L NaClO solution for 15 s, followed by draining with sterile gauze at room temperature. The shredded potatoes were then divided into two groups. The control group was immersed in deionized water for 4 min at room temperature, whereas the Glu group was immersed in a 15 g/L Glu solution for 4 min under the same conditions. Subsequently, all samples were stored at 4 °C for subsequent analysis. Each group consisted of three biological replicates. Samples were collected at 0 (before treatment), 12, 24, 48 and 72 h and stored at −80 °C.

Ethylene production

For measuring ethylene production, 500 g of fresh-cut potatoes from the control and Glu groups were separately placed in an airtight container equipped with a rubber stopper for 2 h at 25 °C. Subsequently, 1 mL of the headspace gas was collected from each sample in triplicate for determining ethylene. Ethylene production was measured by the method of Zhu et al.[35].

Transcription level analysis

Reverse transcription–quantitative polymerase chain reaction (RT-qPCR) was performed, following the protocol of Guan et al.[3]. Briefly, total RNA was extracted from different fresh-cut potatoes using the FastPure Universal Plant Total RNA Isolation Kit and reverse-transcribed into cDNA with the EVO M-MLV Kit. Gene transcription levels were calculated by the $2^{-\Delta\Delta CT}$ method[36], using *β-actin* as the internal reference gene[3].

Sequencing and gene annotation

RNA-Seq analysis was carried out according to Guan et al.[3]. Briefly, fresh-cut potatoes treated with or without Glu at 0 (before treatment), 12 and 48 h were analyzed by RNA-Seq with three biological replicates per time point. All cDNA libraries were sequenced and analyzed by OE Biotechnology Co., Ltd. (Shanghai, China) on an Illumina Hi-Seq 2500 platform.

Prior to downstream analysis, clean reads from each sample were mapped to the potato reference genome database (www.ncbi.nlm.nih.gov/datasets/genome/?taxon=4113) using TopHat2 software. A heatmap was generated with Tbtools, and differentially expressed genes (DEGs) were identified via clustered profile analysis with thresholds of $p \leq 0.05$ and a fold-change of ≥ 2.

Subcellular localization assay

The full coding sequences (CDSs) of *StbZIP53-like2* and *StERF091* were cloned into the pBE-GFP vector to obtain StbZIP53-like2-GFP and StERF091-GFP vectors. Then the StbZIP53-like2-GFP, StERF091-GFP and pBE-GFP vectors were individually expressed in tobacco (*Nicotiana benthamina*) leaves by *Agrobacterium tumefaciens* mediation. After 36–48 h, the green fluorescence protein (GFP) signals in the tobacco leaves were detected using a fluorescence microscope (Zeiss Axioskop 2 Plus, Leica, Solms, Germany) at 488 nm[3].

Yeast two-hybrid assay

The CDSs of *StbZIP53-like2* and *StERF091* were separately cloned into pGBKT7 and pGADT7 to construct the AD-StbZIP53-like2, AD-StERF091, BD-StbZIP53-like2 and BD-StERF091 vectors. Sequentially, AD-StbZIP53-like2 + BD-StERF091 and BD-StbZIP53-like2 + AD-StERF091 were expressed in yeast strains to confirm their interaction. The transformed yeast strains were grown at 28 °C on a culture medium without adenine (Ade), histidine (His), tryptophan (Trp) and leucine (Leu), and the interaction of StbZIP53-like2 and StERF091 were tested according to their growth status and α-galactosidase activity. Recombinants of T-antigen + lamin and T-antigen + P53, respectively, served as the negative and positive controls.

GST pull-down assay

The CDS of *StbZIP53-like2* was cloned into the pGEX-4T-1 vector to get GST-StbZIP53-like2 recombinant proteins, which were induced with 0.1 mM isopropyl-β-D-thiogalactopyranoside (IPTG) at 16 °C for 16 h. Moreover, the CDS of *StERF091* was cloned into the PET-28a vector to get His-StERF091 recombinant proteins, which were induced with 0.2 mM IPTG at 28 °C for 6 h. GST-StbZIP53-like2 and His-StERF091 proteins were purified according to Song et al.[33]. His-StERF091 was then incubated with gutathione S-transferase (GST) or GST-StbZIP53-like2, and their interaction was detected by Western blotting using anti-His antibodies and anti-GST antibodies (Huaan, Shenzhen, China).

Co-immunoprecipitation assay

The CDS of *StERF091* was inserted into the pEAQ-HT-GFP vector, and the CDS of *StbZIP53-like2* was ligated to the PBI121-Flag vector.

The recombinant vectors were then infiltrated into 6-week-old tobacco leaves using *A. tumefaciens* GV3101. After 48 h of infiltration, the protein was extracted from tobacco leaves and reacted with the anti-GFP rabbit antibody (Cat. No. ab290, Abcam, Cambridge, UK) for 2 h. Then the protein A agarose beads were mixed and incubated for 4 h and washed four times before the the beads were collected for Western blot analysis using anti-Flag (Cat. No. 3165, Sigma) and anti-GFP (Cat. No. ab290, Abcam).

Transient dual luciferase expression assay

The CDSs of *StbZIP53-like2* and *StERF091* were separately cloned into the pGreenII62-SK vector to serve as effector constructs, whereas the promoter regions of *StPPO2*, *StPPO3* and *StPPO7* were cloned separately into the pGreenII-0800-LUC vector as reporter plasmids. Subsequently, the reporter and effector vectors were co-expressed in tobacco leaf tissues by *A. tumefaciens* mediation. Following 48 h of expression, luciferase activity was determined in accordance with the protocol provided by the Dual Luciferase Assay Kit (Promega, Madison, WI, USA). Each dual luciferase reporter assay was conducted with six replicates, and the resulting data are presented as the firefly luciferase/renilla luciferase (LUC/REN) ratio.

Yeast one-hybrid library assay

AD-StbZIP53-like2 and AD-StERF091 were obtained as described above. The promoter sequences of *StPPO2* and *StPPO3* were separately cloned into the pBait-ABAi vector to generate bait plasmids, which were subsequently transduced into the yeast one-hybrid (Y1H) Gold strain. To verify the binding affinity, the AD-StbZIP53-like2 and AD-StERF091 vectors were separately introduced into the bait–reporter yeast strain, and their interaction was validated. Protein–DNA interactions were assessed on the basis of the growth status of co-transformed yeast cells on SD/-Leu medium supplemented with Aureobasidin A (AbA).

Electrophoretic mobility shift assay

The CDS of *StERF091* was inserted into the pGEX-4T-1 vector to get GST-StERF091 recombinant proteins, which were induced with 0.1 mM IPTG at 16 °C for 16 h. The recombinant protein was purified according to Guan et al.[3]. The GST-StbZIP53-like2 protein was obtained as described above. Probes of *StPPO2* and *StPPO3* were labeled at the 3' end via the method of Guan et al.[3]. Unlabeled wild-type promoter fragments containing the GCC-box or C-box were used as competitors, whereas mutant probes with the GCC-box or C-box replaced by AAAAAA served as negative controls. The electrophoretic mobility shift assay (EMSA) was conducted according to Guan et al.[3].

Statistical analysis

All experiments were performed with three or six independent biological replicates. Data were analyzed with Duncan's multiple range test using SPSS 25 or the *t*-test, and the results are presented as the mean ± standard deviation (SD). All primers are listed in Supplementary Table S1.

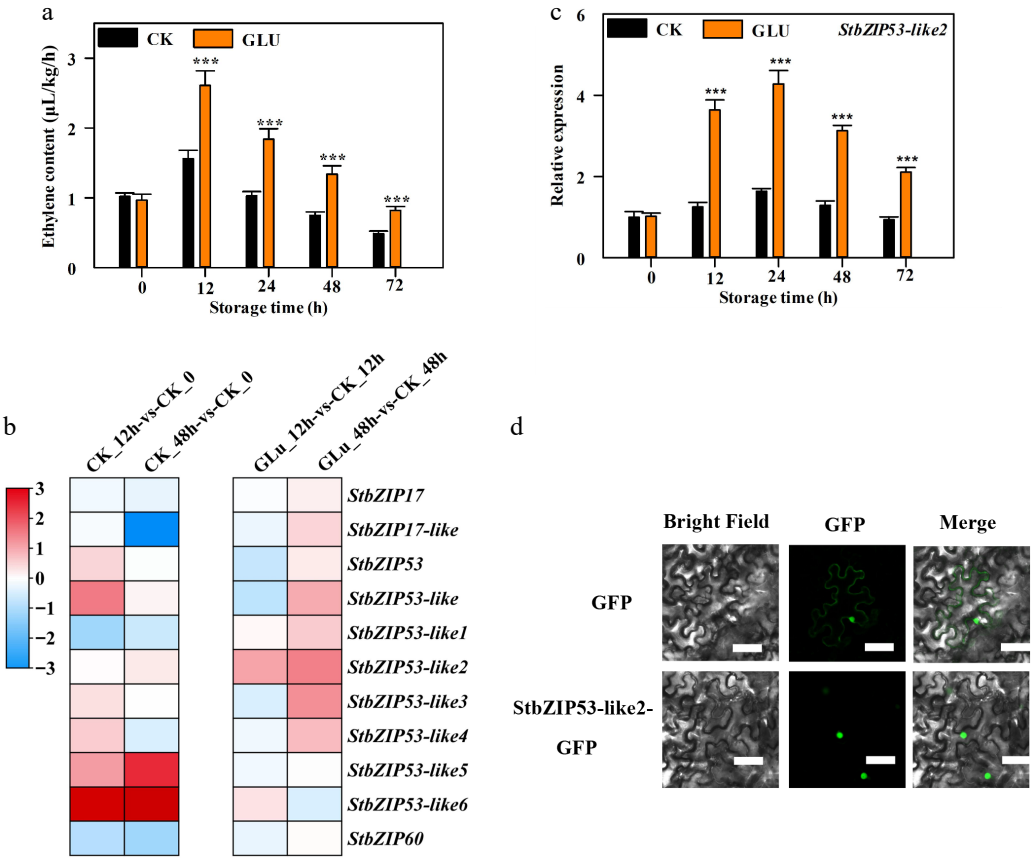

Fig. 1 Ethylene content and the expression and subcellular location of *StbZIP53-like2*. (a) Ethylene content. (b) Expression profiles of 11 StbZIP genes in the RNA-Seq analysis during storage. (c) The expression of *StbZIP53-like2*. The expression levels of *StbZIP53-like2* at different points are relative to 0 h, which was set as 1. *** indicates a significant difference at $p < 0.001$. (d) The subcellular location of *StbZIP53-like2*. Bars = 50 μm.

Results

The expression of StbZIP53-like2 was enhanced by Glu treatment

As shown in Fig. 1a, ethylene content increased first and then decreased, and Glu treatment significantly induced its content. Eleven bZIP genes with differences in expression were identified by our RNA-Seq analysis. The expression of *StbZIP17*, *StbZIP17-like*, *StbZIP53-like1* and *StbZIP60* was reduced with incrased storage time, and the expression of *StbZIP53*, *StbZIP53-like*, *StbZIP53-like2*, *StbZIP53-like3*, *StbZIP53-like5* and *StbZIP53-like6* was increased with increased storage time. The expression of *StbZIP17*, *StbZIP17-like*, *StbZIP53*, *StbZIP53-like*, *StbZIP53-like3*, *StbZIP53-like4* and *StbZIP60* was inhibited by Glu treatment at 12 h but was enhanced by Glu treatment at 24 h. However, the expression of *StbZIP53-like6* was induced by Glu treatment at 12 h but was repressed by Glu treatment at 24 h. Moreover, only the expression of *StbZIP53-like1* and *StbZIP53-like2* was induced by Glu treatment at both 12 h and 24 h, and the expression level of *StbZIP53-like2* was the highest (Fig. 1b). Thus, it was selected for further study. RT-qPCR analysis confirmed this result, showing that the expression first increased and then decreased, and that Glu treatment markedly induced its expression (Fig. 1c). Moreover, StbZIP53-like2 contains 166 amino acids and a bZIP_plant_GBF1 domain (Supplementary Fig. S1) and is located in the nucleus (Fig. 1d).

StbZIP53-like2 mediates the expression of StPPO3

Our previous study found that the transcription of *StPPO2*, *StPPO3* and *StPPO7* was closely related to the browning of fresh-cut potatoes[3]. Therefore, we aimed to find out whether the expression of *StPPO2*, *StPPO3* and *StPPO7* was regulated by StbZIP53-like2. A DLR assay was performed; the promoters of *StPPO2*, *StPPO3* and *StPPO7* were separately cloned into pGreenII 0800-LUC effector vector; and the CDS of *StbZIP53-like2* was cloned into the pGreenII 62-SK reporter vector (Fig. 2a). The promoter activity of *StPPO3* was severely repressed by StbZIP53-like2, but the promoters of *StPPO2* and *StPPO7* were not regulated by StbZIP53-like2 (Fig. 2b). EMSA was used to verify StbZIP53-like2 binding of the promoter of *StPPO3*. The data indicated that GST-StbZIP53-like2 could directly interact with the C-box motif of *StPPO3* and caused mobility shifts, but GST protein alone did not cause a mobility shift. Moreover, the shifted bands were reduced when the unlabeled competitor increased, but not the mutant probes (Fig. 2c). In addition, the Y1H assay further verified that StbZIP53-like2 could directly bind to *StPPO3* (Fig. 2d). These results indicated that StbZIP53-like2 inhibited the expression of *StPPO3* by directly and specifically interacting with the C-box motif.

StbZIP53-like2 interacts with StERF091

We aimed to detect whether StbZIP53-like2 interacts with other proteins in the browning of fresh-cut potatoes. As shown in

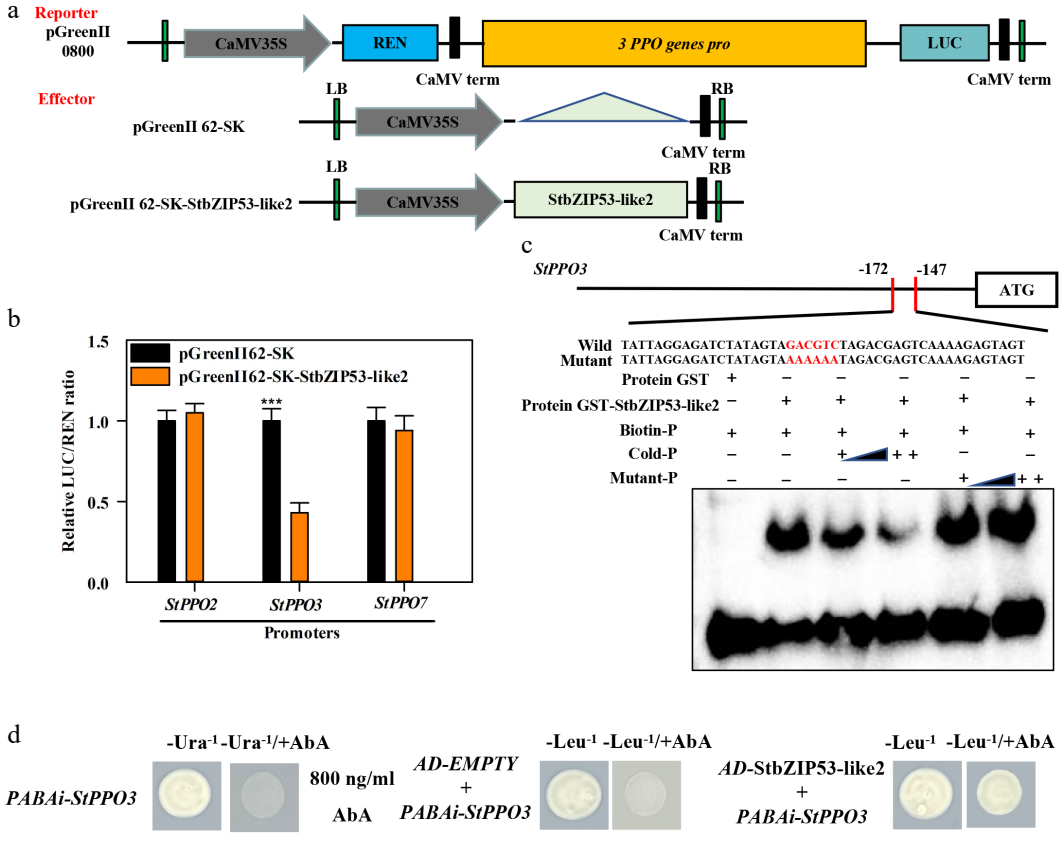

Fig. 2 Effect of StbZIP53-like2 mediates the transcriptional activity of *StPPO2*, *StPPO3* and *StPPO7*. (a) Picture of the reporters and the effector. (b) The promoter activity of *StPPO2*, *StPPO3* and *StPPO7* was regulated by StbZIP53-like2. The empty vector co-expressed with promoters was used as a control (set as 1). *** indicates a significant difference at $p < 0.001$. (c) The cooperation of StbZIP53-like2 with the promoter of *StPPO3* in the EMSAs. GST-StbZIP53-like2 protein was mixed with the probes of *StPPO3* including the C-box motif and the mutant probes AAAAAA, which are shown in red letters. ++ indicates increasing amounts of the probe; – represents absence; + represents presence. (d) StbZIP53-like2 interacts with the promoter of *StPPO3 in vivo*. Yeast growth assays indicated the interaction of StbZIP53-like2 with the promoters of *StPPO3*.

Supplementary Fig. S2, BD-StbZIP53-like2 does not have self-activation ability, and it was used to screen the cDNA library. StERF091 protein was identified. The yeast two-hybrid assay (Y2H data) indicated that BD-StERF091 also does not have self-activation ability, and StERF091 interacted with StbZIP53-like2 in the yeast strain (Fig. 3a). In addition, GST-StbZIP53-like2 could reduce His-StERF091 but not GST protein, which indicated that StERF091 cooperated with StbZIP53-like2 *in vitro* (Fig. 3b). Moreover, the co-immunoprecipitation (Co-IP) assay also indicated that StERF091 could immunoprecipitate StbZIP53-like2 protein. The data indicated that StERF091 interacted with StbZIP53-like2 *in vitro* and *in vivo*.

Glu induced StERF091 expression and repressed StPPO2 and StPPO3 expression

The expression of *StERF091* first increased and then decreased, which was enhanced by Glu treatment (Fig. 4a). Moreover, StERF091 contained 261 amino acids and the AP2 domain (Supplementary Fig. S3) and it was located in the nucleus (Fig. 4b).

To detected whether StERF091 mediates the promoter activity of *StPPO2*, *StPPO3* and *StPPO7*, a DLR assay was performed. The promoters of *StPPO2*, *StPPO3* and *StPPO7* were separately cloned into the pGreenII 0800-LUC reporter vector, and the CDS of *StERF091* was cloned into the pGreenII 62-SK effector vector (Fig. 5a). The promoter activity of *StPPO2* and *StPPO3* was severely repressed by StERF091, but the promoter of *StPPO7* was not regulated by StERF091 (Fig. 5b). EMSA was used to verify whether StERF091 bound the promoter of *StPPO2* and *StPPO3*. The data indicated that GST-StERF091 could directly interact with the GCC-box motif of *StPPO2* and *StPPO3* and caused mobility shifts, but GST protein alone did not cause a mobility shift. Moreover, the shifted bands were reduced as the unlabeled competitor increased, but not the mutant probes (Fig. 5c). Additionally, the Y1H assay further verified that StERF091 could directly bind to *StPPO2* and *StPPO3* (Fig. 5d). These results indicated that StERF091 inhibited the expression of *StPPO2* and *StPPO3* by directly and specifically interacting with the GCC-box motif.

StbZIP53-like2 interacted with StERF091 to inhibit StPPO2 and StPPO3 expression

The above data indicated that StbZIP53-like2 interacted with StERF091, StbZIP53-like2 repressed *StPPO3* expression and StERF091 repressed *StPPO2* and *StPPO3* expression. Therefore, we explored whether the cooperation of StbZIP53-like2 and StERF091 affects the regulation of its downstream genes. The DLR results showed that when StbZIP53-like2 and StERF091 were co-expressed in tobacco leaves, the transcriptional activity of *StPPO2* and *StPPO3* was lower than when StbZIP53-like2 or StERF091 was expressed alone (Fig. 6).

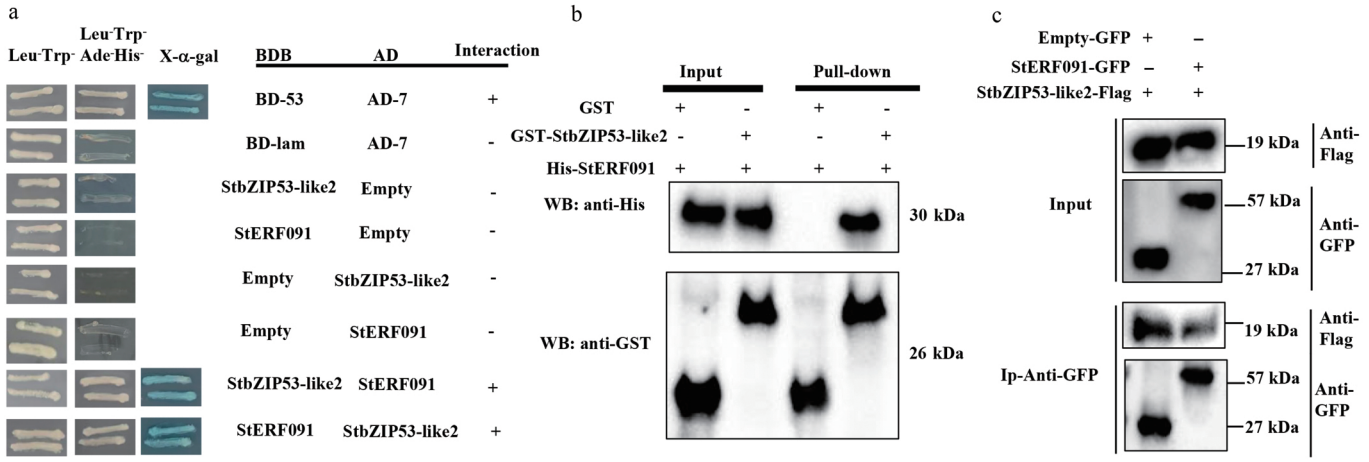

Fig. 3 The cooperation between StbZIP53-like2 and StERF091 proteins. (a) The Y2H assay confirmed the cooperation of StbZIP53-like2 and StERF091. Yeast cells grew on SD/-Leu$^-$Trp$^-$Ade$^-$His$^-$ with 125 μM Aureobasidin A and turned blue in the presence of 4 mg/mL X-α-Gal; this served as a positive interaction. (b) GST pull-down assay of the cooperation between StbZIP53-like2 and StERF091. His-StERF091 protein was incubated with GST-StbZIP53-like2 or GST. The anti-His antibody and anti-GST antibody were used for the immunoblotting assays. (c) The co-immunoprecipitation assay confirmed the interaction between StbZIP53-like2 and StERF091. Here, – represents the absence and + represents the presence of the fusion proteins. The anti-Flag and anti-GFP antibodies were used for immunoprecipitation.

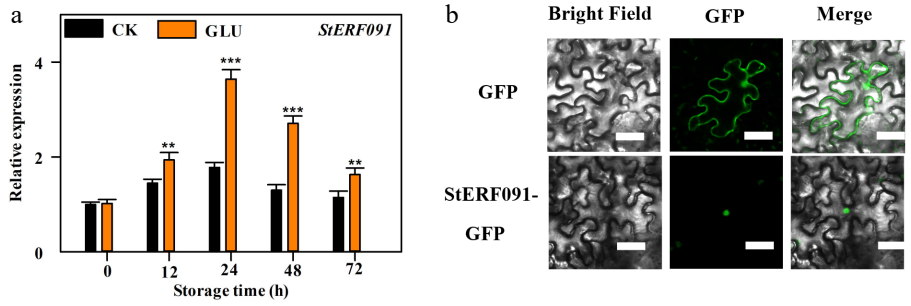

Fig. 4 The expression and subcellular location of *StERF091*. (a) The expression of *StERF091*. The expression levels of *StERF091* at different points are relative to 0 h, set as 1. ** and *** indicate significant differences at $p < 0.01$ and $p < 0.001$, respectively. (b) The subcellular location of *StERF091*. Bars = 50 μm.

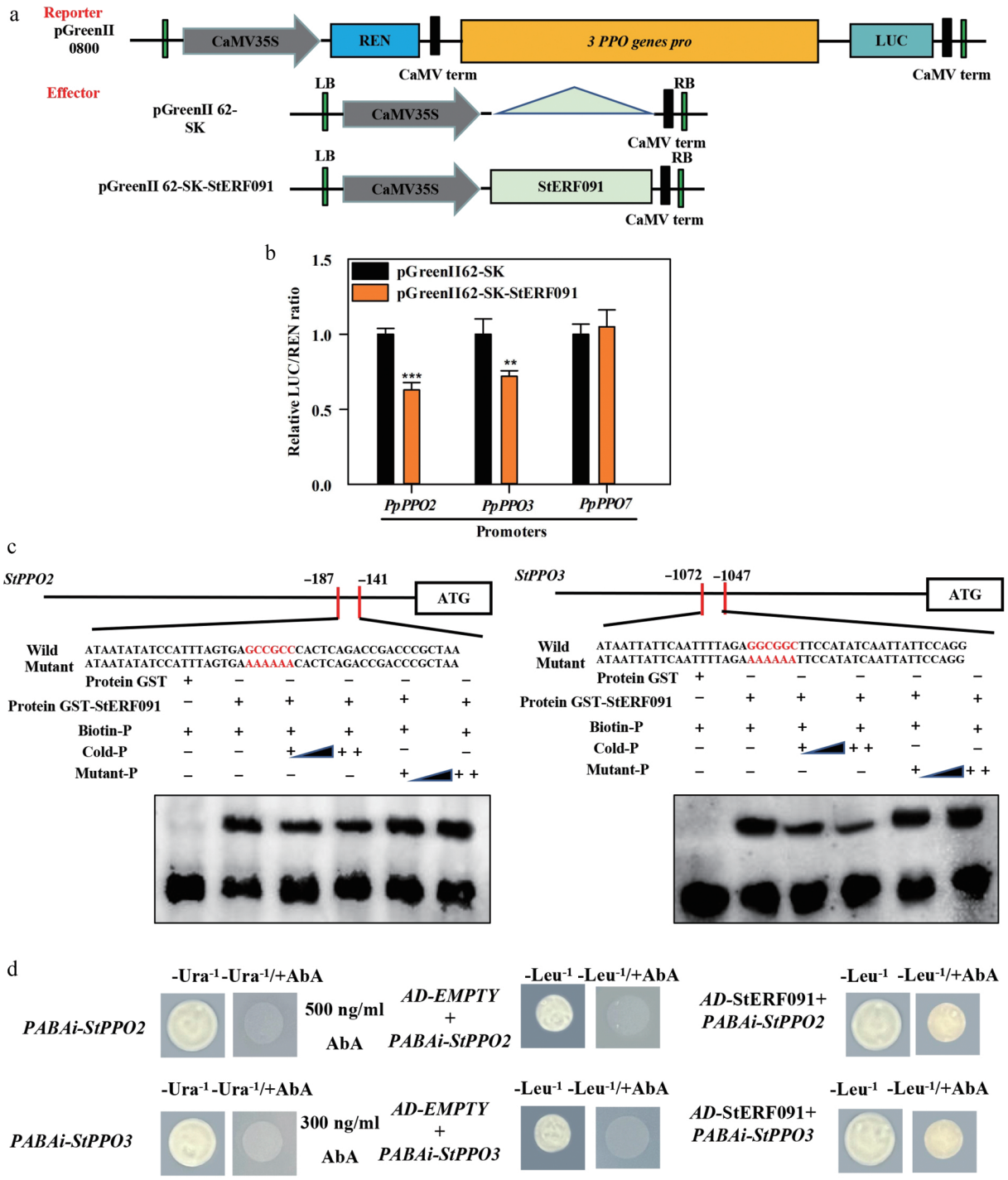

Fig. 5 StERF091 mediates the transcriptional activity of *StPPO2*, *StPPO3* and *StPPO7*. (a) Picture of the reporters and the effector. (b) The promoter activity of *StPPO2*, *StPPO3* and *StPPO7* was regulated by StERF091. The empty vector co-expressed with the promoters was used as a control (set as 1). ** and *** indicate significant differences at $p < 0.01$ and $p < 0.001$. (c) The cooperation of StERF091 with the promoter of *StPPO2* and *StPPO3* in EMSAs. GST-StERF091 protein was mixed with the probes of *StPPO2* and *StPPO3* including the GCC-box motif and the mutant probes AAAAAA (shown in red letters). ++ indicates increasing amounts of the probe, – represents absence and + represents presence. (d) StERF091 interacts with the promoter of *StPPO2* and *StPPO3 in vivo*. Yeast growth assays indicated the interaction of StERF091 with the promoters of *StPPO2* and *StPPO3*.

Discussion

The browning of fruit and vegetables severely reduces its commercial value. TFs play a key role in regulating the browning of vegetables and fruit. PuMYB21 and PuMYB24 regulate the peel-browning of 'Nanguo' pear by stimulating the transcriptional activity of *PuPLDβ1* by directly binding to its promoter[37]. CAMTA5 alleviates the browning of loquat (*Eriobotrya japonica*) fruit by inhibiting the expression of *EjLOX5* and *EjPLC6-like*, which are the key genes in membrane lipid metabolism[38]. In pineapple (*Ananas comosus*), AcbHLH144 represses the internal browning of fruit by inhibiting transcription of the phenolic biosynthesis gene *Ac4CL5*[39]. In peach, PpERF17 alleviates fruit browning by activating the jasmonic acid (JA) signaling pathway[40]. In banana, transient overexpression of *MaWRKY18/33/40/60* significantly increases browning of

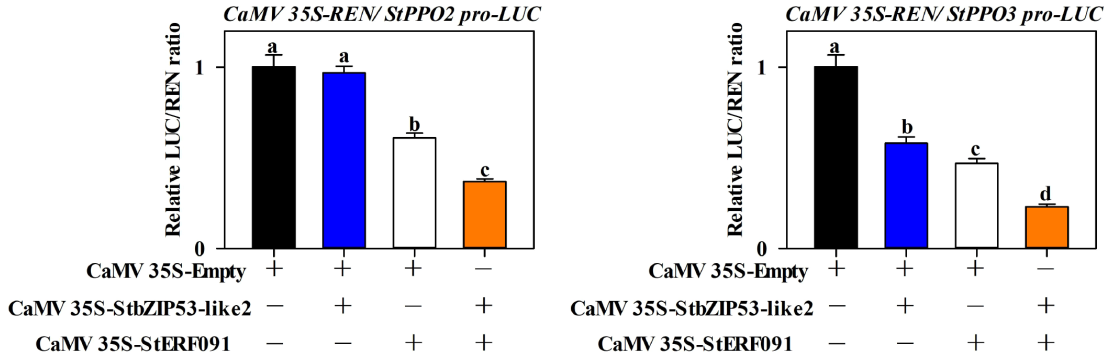

Fig. 6 Combinatory effects of StbZIP53-like2 and StERF091 in mediating the expression of *StPPO2* and *StPPO3*. The empty vector co-expressed with the promoters was used as a control (set as 1). The letters a, b, c and d indicate significant differences at $p < 0.05$.

the fruit peel[41]. In apple, MdHY5 and MdHYH inhibits fruit browning by repressing the expression of *MdPOD* and *MdPPO*, and enhances *MdPAL* expression[42]. MdWRKY31 increases the browning of fruit by stimulating the transcription of *MdLAC7*[43], and MdWRKY3 also enhances the browning of fruit by activating *MdPPO7* expression[44]. All this information indicates that there is a complex of transcriptional regulation acting in the browning of fruit and vegetables.

Some research has reported that bZIP TFs regulate fruit and vegetable browning. JrbZIP55, JrbZIP70, JrbZIP72 and JrbZIP88 play a key role in explant browning[45]. In apple, MdbZIP44 aggravates the browning of fruit by stimulating the expression of *MdPPO2*[46]. However, how bZIP TFs regulate the browning of fresh-cut fruit and vegetables was not reported. Herein, the data first identified the bZIP TF StbZIP53-like2, whose expression was enhanced by the Glu treatment, and StbZIP53-like2 could repress the expression of *StPPO3* by directly binding its promoter (Figs 1 and 2).

Plant hormones play a key role in fruits' development, maturation and ripening. Ethylene promotes fruit ripening in banana, tomato and papaya (*Carica papaya*)[47]. Additionally, some studies found that ethylene also affects the ripening of fresh-cut fruit and vegetables. For example, ethylene represses the internal browning of 'Gala' apples[48]. Ethylene inhibits the peel browning of 'Huangguan' pear by inhibiting the activity of PPO[49]. The browning of 'Yali' pear was reduced by reducing ethylene production[50]. However, ethylene also induces the browning of fruit and vegetables. For example, ethylene induces the browning of pomegranate (*Punica granatum*) peel by regulating the antioxidant and fatty acid content[51]. Ethylene increases the browning of apple fruit flesh by inducing the expression of *MdPPO* and *MdERF106*[52]. In this study, Glu treatment enhanced the ethylene content in fresh-cut potato (Fig. 1). Moreover, several studies have reported that ERFs regulate fruit and vegetable browning. NnERF4/5 were the main regulators in regulating the browning of fresh-cut lotus root[53]. Our previous study found that StERF-BR1-like positively regulates *StPPO2* expression by directly binding its promoter, and the expression of *StERF-BR1-like* was repressed by Glu treatment[3]. In this study, the expression of *StERF091* was increased by Glu treatment, and StERF091 significantly inhibited the expression of *StPPO2* and *StPPO3* by directly binding their promoter (Figs 4 and 5). All these data indicate that Glu treatment alleviates the browning of fresh-cut potatoes by enhancing the expression of StbZIP53-like2 and StERF091, which further inhibits the expression of *StPPO2* and *StPPO3*.

Protein interactions play a key role in fruit and vegetable development, maturation and resistance to biotic and abiotic stresses. In peach, PpERF5 interacts with PpERF7 and enhances fruit aroma by activating *PpLOX4* transcription[34]. PpZAT6 cooperates with

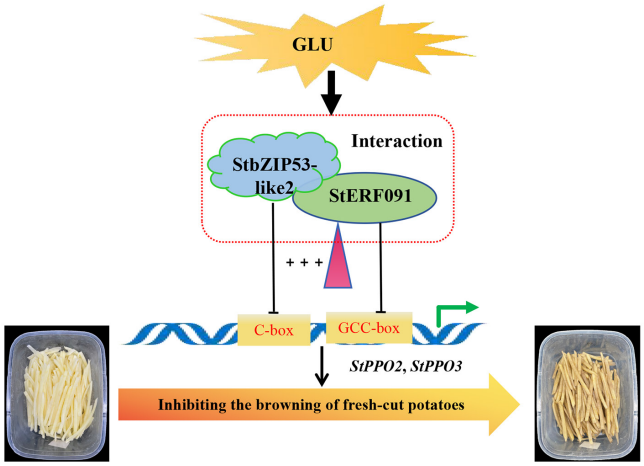

Fig. 7 Glu alleviates the browning of fresh-cut potatoes by enhancing the expression of StbZIP53-like2 and StERF091, thus inhibiting the transcriptional activity of *StPPO2* and *StPPO3*.

PpWRKY46 to form a complex enhancing the fruit's cold tolerance by activating the expression of proline synthesis genes[54]. PpWRKY22 cooperates with PpWRKY70 to form a complex improve fruits' resistance to *Monilinia fructicola* by enhancing the gamma-aminobutyric acid shunt[55]. In banana, MaEBF1 interacts with MaABI5-like to enhance MaABI5-like, regulating starch and cell degradation[56]. In tomato, SlWRKY42 interacts with SlMYC2, and increased SlWRKY42 regulates *SlSPDS2* expression and promotes spermidine accumulation[57]. In lychee (*Litchi chinensis*), LcWRKY1 interacts with LcNAC1 to form a complex regulating *LcAOX1* expression[58]. In apple, MdWRKY41 cooperates with MdMYB16 to form a complex to regulate anthocyanin and proanthocyanidin biosynthesis by repressing the expression of *MdANR* and *MdUFGT*[59]. Moreover, protein interactions also affects TFs regulating the browning of fruit and vegetables. PuMYB21 interacts with PuMYB24, and this interaction mediates the browning of 'Nanguo' pear by enhancing the transcription of *PuPLDβ1*[37]. However, protein interactions mediating the browning of fresh-cut fruit and vegetables are not yet widely reported. In this study, the data shown that StbZIP53-like2 interacts with StERF091 to form a complex to mediate the browning of fresh-cut potatoes by inhibiting the expression of *StPPO2* and *StPPO3* (Fig. 6).

Conclusions

This study found two new transcription repressors, StbZIP53-like2 and StERF091, whose transcription was enhanced by Glu treatment.

StbZIP53-like2 repressed the expression of *StPPO3,* and StERF091 repressed the expression of *StPPO2* and *StPPO3* by directly interacting with their promoters. Additionally, StbZIP53-like2 interacts with StERF091 to form a complex, which enhanced the inhibition of *StPPO2* and *StPPO3*, thereby alleviating the browning of fresh-cut potatoes (Fig. 7). Taken together, the data uncover a StbZIP53-like2–StERF091 module that alleviates the browning of fresh-cut potatoes under Glu treatment.

Author contributions

The authors confirm their contributions to the paper as follows: methodology, formal analysis, draft manuscript preparation: Li W; data curation: Li W, Cao J, He Y, Wang Y; investigation: Li W, Cao J; validation: Cao J, Shi J, Song Z; conceptualization, writing – review & editing, supervision, resources: Shi J, Song Z. All authors reviewed the results and approved the final version of the manuscript.

Data availability

The datasets generated during and/or analyzed in the current study are available from the corresponding author on reasonable request.

Acknowledgments

This work was supported by the Natural Science Foundation of Shandong Province (ZR2023QC010), the Key R & D project of Shandong Province (Grant No. 2021TZXD007) and the Potato Industry Innovation Team for Modern Agricultural Industry Technology System of Shandong Province (SDAIT-16-11).

Conflict of interest

The authors declare that they have no conflict of interest.

Supplementary information accompanies this paper online at: https://doi.org/10.48130/ph-0026-0004.

Dates

Received 20 January 2026; Revised 7 February 2026; Accepted 24 February 2026; Published online 20 March 2026

References

[1] Zhou F, Jiang A, Feng K, Gu S, Xu D, et al. 2019. Effect of methyl jasmonate on wound healing and resistance in fresh-cut potato cubes. *Postharvest Biology and Technology* 157:110958

[2] Ma Y, Wang H, Yan H, Malik AU, Dong T, et al. 2021. Pre-cut NaCl solution treatment effectively inhibited the browning of fresh-cut potato by influencing polyphenol oxidase activity and several free amino acids contents. *Postharvest Biology and Technology* 178(1):111543

[3] Guan Q, Li W, Dai M, Qiao J, Wu B, et al. 2025. Key factors uncovered by transcriptomic analysis in the regulation of glutamic acid repressing the browning of fresh-cut potatoes. *Postharvest Biology and Technology* 219:113242

[4] Liu X, Wang T, Lu Y, Yang Q, Li Y, et al. 2019. Effect of high oxygen pretreatment of whole tuber on anti-browning of fresh-cut potato slices during storage. *Food Chemistry* 301:125287

[5] Song Z, Qiao J, Tian D, Dai M, Guan Q, et al. 2023. Glutamic acid can prevent the browning of fresh-cut potatoes by inhibiting PPO activity and regulating amino acid metabolism. *Lwt* 180:114735

[6] Feng Y, Liu Q, Liu P, Shi J, Wang Q. 2020. Aspartic acid can effectively prevent the enzymatic browning of potato by regulating the generation and transformation of brown product. *Postharvest Biology and Technology* 166:111209

[7] Meng Z, Wang T, Malik AU, Wang Q. 2022. Exogenous isoleucine can confer browning resistance on fresh-cut potato by suppressing polyphenol oxidase activity and improving the antioxidant capacity. *Postharvest Biology and Technology* 184:111772

[8] Zhou X, Xiao Y, Meng X, Liu B. 2018. Full inhibition of Whangkeumbae pear polyphenol oxidase enzymatic browning reaction by l-cysteine. *Food Chemistry* 266:1–8

[9] Prabasari I, Utama NA, Wijayanti EP, Hasanah NAU, Riyadi S, et al. 2020. L-Arginine to inhibit browning on fresh-cut salacca (*Salacca edulis* Reinw). *IOP Conference Series: Earth and Environmental Science* 458:012027

[10] Yuan H, Liu Y, Zhang J, Dong JF, Zhao Z. 2023. Transcription factors in megakaryocytes and platelets. *Frontiers in Immunology* 14:1140501

[11] Wu C, Shan W, Liang S, Zhu L, Guo Y, et al. 2019. MaMPK2 enhances MabZIP93-mediated transcriptional activation of cell wall modifying genes during banana fruit ripening. *Plant Molecular Biology* 101(1):113–127

[12] Aslam MM, Deng L, Meng J, Wang Y, Pan L, et al. 2023. Characterization and expression analysis of basic leucine zipper (bZIP) transcription factors responsive to chilling injury in peach fruit. *Molecular Biology Reports* 50(1):361–376

[13] Chen M, Cao X, Huang Y, Zou W, Liang X, et al. 2024. The bZIP transcription factor MpbZIP9 regulates anthocyanin biosynthesis in *Malus* 'Pinkspire' fruit. *Plant Science* 342:112038

[14] Sun Q, He Z, Wei R, Zhang Y, Ye J, et al. 2024. The transcriptional regulatory module CsHB5-CsbZIP44 positively regulates abscisic acid-mediated carotenoid biosynthesis in citrus (*Citrus* spp.). *Plant Biotechnology Journal* 22(3):722–737

[15] Yang M, Song C, Lin Y, Zhang Y, Li M, et al. 2025. FaTRAB1, a bZIP transcription factor, enhances anthocyanin biosynthesis in strawberry leaves via tissue-specific regulation. *PLoS Genetics* 21(9):e1011888

[16] Wang H, Xu K, Li X, Blanco-Ulate B, Yang Q, et al. 2023. A pear S1-bZIP transcription factor PpbZIP44 modulates carbohydrate metabolism, amino acid, and flavonoid accumulation in fruits. *Horticulture Research* 10(8):uhad140

[17] Jia L, Zhang X, Zhang Z, Luo W, Nambeesan SU, et al. 2024. PbrbZIP15 promotes sugar accumulation in pear via activating the transcription of the glucose isomerase gene *PbrXylA1*. *The Plant Journal* 117(5):1392–1412

[18] Wu CJ, Shan W, Liu XC, Zhu LS, Wei W, et al. 2022. Phosphorylation of transcription factor bZIP21 by MAP kinase MPK6-3 enhances banana fruit ripening. *Plant Physiology* 188(3):1665–1685

[19] Gai S, Du B, Xiao Y, Zhang X, Turupu M, et al. 2024. bZIP transcription factor PavbZIP6 regulates anthocyanin accumulation by increasing abscisic acid in sweet cherry. *International Journal of Molecular Sciences* 25(18):10207

[20] Li S, Wu P, Yu X, Cao J, Chen X, et al. 2022. Contrasting roles of ethylene response factors in pathogen response and ripening in fleshy fruit. *Cells* 11(16):2484

[21] Deng H, Chen Y, Liu Z, Liu Z, Shu P, et al. 2022. SlERF.F12 modulates the transition to ripening in tomato fruit by recruiting the co-repressor TOPLESS and histone deacetylases to repress key ripening genes. *The Plant Cell* 34(4):1250–1272

[22] Hu K, Geng M, Ma L, Yao G, Zhang M, et al. 2025. The H_2S-responsive transcription factor ERF.D3 regulates tomato abscisic acid metabolism, leaf senescence, and fruit ripening. *Plant Physiology* 197(2):kiae560

[23] Guo H, Mao M, Deng Y, Sun L, Chen R, et al. 2022. Multi-omics analysis reveals that *SlERF.D6* synergistically regulates SGAs and fruit development. *Frontiers in Plant Science* 13:860577

[24] Gambhir P, Singh V, Parida A, Raghuvanshi U, Kumar R, et al. 2022. Ethylene response factor ERF. D7 activates auxin response factor 2 paralogs to regulate tomato fruit ripening. *Plant Physiology* 190(4):2775–2796

[25] Deng H, Pei Y, Xu X, Du X, Xue Q, et al. 2024. Ethylene-MPK8-ERF.C1-PR module confers resistance against *Botrytis cinerea* in tomato fruit without compromising ripening. *The New Phytologist* 242(2):592–609

[26] Qi X, Liu L, Liu C, Song L, Dong Y, et al. 2023. Sweet cherry AP2/ERF transcription factor, PavRAV2, negatively modulates fruit size by directly repressing *PavKLUH* expression. *Physiologia Plantarum* 175(6):e14065
[27] An JP, Zhang XW, Bi SQ, You CX, Wang XF, et al. 2020. The ERF transcription factor MdERF38 promotes drought stress-induced anthocyanin biosynthesis in apple. *The Plant Journal* 101(3):573–589
[28] Li T, Liu Z, Lv T, Xu Y, Wei Y, et al. 2023. Phosphorylation of MdCYTOKININ RESPONSE FACTOR4 suppresses ethylene biosynthesis during apple fruit ripening. *Plant Physiology* 191(1):694–714
[29] Rui L, Zhu ZQ, Yang YY, Wang DR, Liu HF, et al. 2023. Functional characterization of MdERF113 in apple. *Physiologia Plantarum* 175(1):e13853
[30] Xie WS, Xiao YY, Wei W, Shan W, Kuang JF, et al. 2026. Methionine oxidation-regulated MaERF95L controls starch and sucrose metabolism in postharvest banana during ripening. *Journal of Integrative Plant Biology* 68(2):439–454
[31] Song Z, Li W, Chen H, Shi J, Zhu H, et al. 2025. E3 ligase SINAT5 mediates ERF113 stability and negatively governs the module of ABI5-like-ERF113 in regulating banana fruit ripening. *New Phytologist* 248(3):1284–1303
[32] Song Z, Chen H, Zhao Y, Wang L, Chen W, et al. 2025. The regulatory MaIAA1-like-MaERF003 module modulates the ripening of 'Fenjiao' bananas. *Plant Physiology* 199(4):kiaf595
[33] Wang X, Zhang C, Miao Y, Deng L, Zhang B, et al. 2022. Interaction between PpERF5 and PpERF7 enhances peach fruit aroma by upregulating *PpLOX4* expression. *Plant Physiology and Biochemistry* 185:378–389
[34] Lee JG, Yi G, Seo J, Kang BC, Choi JH, et al. 2020. Jasmonic acid and ERF family genes are involved in chilling sensitivity and seed browning of pepper fruit after harvest. *Scientific Reports* 10:17949
[35] Zhu X, Shen L, Fu D, Si Z, Wu B, et al. 2015. Effects of the combination treatment of 1-MCP and ethylene on the ripening of harvested banana fruit. *Postharvest Biology and Technology* 107:23–32
[36] Livak KJ, Schmittgen TD. 2001. Analysis of relative gene expression data using real-time quantitative PCR and the $2^{-\Delta\Delta CT}$ method. *Methods* 25(4):402–408
[37] Sun HJ, Luo ML, Zhou X, Zhou Q, Sun YY, et al. 2020. PuMYB21/PuMYB54 coordinate to activate *PuPLDβ1* transcription during peel browning of cold-stored 'Nangu' pears. *Horticulture Research* 7:136
[38] Hou Y, Wang L, Zhao L, Xie B, Hu S, et al. 2022. $CaCl_2$ mitigates chilling injury in loquat fruit via the CAMTA5-mediated transcriptional repression of membrane lipid degradation genes. *Food Research International* 162:111966
[39] Li Q, Wang G, Zhang L, Zhu S. 2023. AcbHLH144 transcription factor negatively regulates phenolic biosynthesis to modulate pineapple internal browning. *Horticulture Research* 10(10):uhad185185
[40] Ai S, Liang L, Liu M, Grierson D, Chen K, et al. 2025. PpERF17 alleviates peach fruit postharvest chilling injury under elevated CO_2 by activating jasmonic acid and γ-aminobutyric acid biosynthesis. *Horticulture Research* 12(4):uhaf014
[41] Zhu W, Li H, Dong P, Ni X, Fan M, et al. 2023. Low temperature-induced regulatory network rewiring via WRKY regulators during banana peel browning. *Plant Physiology* 193(1):855–873
[42] Jin J, Qi L, Shen S, Yang S, Yuan H, et al. 2024. Violet LED light-activated MdHY5 positively regulates phenolic accumulation to inhibit fresh-cut apple fruit browning. *Horticulture Research* 12(1):uhae276
[43] Wang H, Zhang S, Fu Q, Wang Z, Liu X, et al. 2023. Transcriptomic and metabolomic analysis reveals a protein module involved in preharvest apple peel browning. *Plant Physiology* 192(3):2102–2122
[44] Zou H, Li C, Wei X, Xiao Q, Tian X, et al. 2024. Expression of the polyphenol oxidase gene *MdPPO7* is modulated by MdWRKY3 to regulate browning in sliced apple fruit. *Plant Physiology* 197(1):kiae614
[45] Wang H, Peng J, Li Y, Xu L, Dai W, et al. 2023. The role of walnut *bZIP* genes in explant browning. *BMC Genomics* 24(1):377
[46] Zhao J, Zou Q, Bao T, Kong M, Gu T, et al. 2024. Transcription factor MdbZIP44 targets the promoter of *MdPPO2* to regulate browning in *Malus domestica* Borkh. *Plant Physiology and Biochemistry* 214:108934
[47] Liu M, Pirrello J, Chervin C, Roustan JP, Bouzayen M. 2015. Ethylene control of fruit ripening: revisiting the complex network of transcriptional regulation. *Plant Physiology* 169(4):2380–2390
[48] DeEll JR, Lum GB, Mostofi Y, Lesage SK. 2022. Timing of ethylene inhibition affects internal browning and quality of 'Gala' apples in long-term low oxygen storage. *Frontiers in Plant Science* 13:914441
[49] Ma Y, Yang M, Wang J, Jiang CZ, Wang Q. 2017. Application of exogenous ethylene inhibits postharvest peel browning of 'Huangguan' pear. *Frontiers in Plant Science* 7:2029
[50] Zhang H, Han Y, Liang L, Deng B. 2024. Rapid cooling delays the occurring of core browning in postharvest 'Yali' pear at advanced maturity by inhibiting ethylene metabolism. *Foods* 13(7):1072
[51] Valdenegro M, Fuentes L, Bernales M, Huidobro C, Monsalve L, et al. 2022. Antioxidant and fatty acid changes in pomegranate peel with induced chilling injury and browning by ethylene during long storage times. *Frontiers in Plant Science* 13:771094
[52] Espley RV, Leif D, Plunkett B, McGhie T, Henry-Kirk R, et al. 2019. Red to brown: an elevated anthocyanic response in apple drives ethylene to advance maturity and fruit flesh browning. *Frontiers in Plant Science* 10:1248
[53] Min T, Liu EC, Xie J, Yi Y, Wang LM, et al. 2019. Effects of vacuum packaging on enzymatic browning and ethylene response factor (ERF) gene expression of fresh-cut lotus root. *HortScience* 54(2):331–336
[54] He Y, Li W, Yang W, Dai M, Shi J, et al. 2025. PpZAT6-PpWRKY46 module regulates chilling stress response of peach fruit by activating proline biosynthesis. *Postharvest Biology and Technology* 230:113733
[55] Li W, Dai M, Wang X, Shi Y, Wang Z, et al. 2025. The PpWRKY22-PpWRKY70 regulatory module enhances resistance to *Monilinia fructicola* by regulating the gamma-aminobutyric acid shunt in peach fruit. *Postharvest Biology and Technology* 220:113306
[56] Song Z, Lai X, Yao Y, Qin J, Ding X, et al. 2022. F-box protein EBF1 and transcription factor ABI5-like regulate banana fruit chilling-induced ripening disorder. *Plant Physiology* 188(2):1312–1334
[57] Liu X, Shang C, Duan P, Yang J, Wang J, et al. 2025. The SlWRKY42-SlMYC2 module synergistically enhances tomato saline-alkali tolerance by activating the jasmonic acid signaling and spermidine biosynthesis pathway. *Journal of Integrative Plant Biology* 67(5):1254–1273
[58] Jiang G, Yan H, Wu F, Zhang D, Zeng W, et al. 2017. Litchi fruit LcNAC1 is a target of LcMYC2 and regulator of fruit senescence through its interaction with LcWRKY1. *Plant & Cell Physiology* 58(6):1075–1089
[59] Mao Z, Jiang H, Wang S, Wang Y, Yu L, et al. 2021. The MdHY5-MdWRKY41-MdMYB transcription factor cascade regulates the anthocyanin and proanthocyanidin biosynthesis in red-fleshed apple. *Plant Science* 306:110848